

# Electron impact excitation of Al XIII: A relativistic approach<sup>\*</sup>

K. M. Aggarwal<sup>1</sup>, F. P. Keenan<sup>1</sup>, and S. J. Rose<sup>2</sup>

<sup>1</sup> Department of Pure and Applied Physics, The Queen's University of Belfast, Belfast BT7 1NN, Northern Ireland, UK  
e-mail: K.Aggarwal@qub.ac.uk

<sup>2</sup> Department of Physics, Clarendon Laboratory, Parks Road, Oxford OX1 3PU, UK

Received 10 November 2004 / Accepted 29 November 2004

**Abstract.** Energy levels, radiative rates, collision strengths, and effective collision strengths for all transitions up to and including the  $n = 5$  levels of Al XIII have been computed in the  $jj$  coupling scheme including relativistic effects. All partial waves with angular momentum  $J \leq 60$  have been included, and resonances have been resolved in a fine energy grid in the threshold region. Collision strengths are tabulated at energies above thresholds in the range  $170.0 \leq E \leq 300.0$  Ryd, and results for effective collision strengths, obtained after integrating the collision strengths over a Maxwellian distribution of electron velocities, are tabulated over a wide temperature range of  $4.4 \leq \log T_e \leq 6.8$  K. The importance of including relativistic effects in a calculation is discussed in comparison with the earlier available non-relativistic results.

**Key words.** atomic data – atomic processes

## 1. Introduction

Atomic data (namely, energy levels, radiative rates, collision strengths, and excitation rate coefficients) for hydrogenic ions are required for the modelling of astrophysical plasmas, as well as for the study of power loss in fusion reactors. Emission lines of Al XIII have been observed in the solar (Phillips et al. 1982) as well as in the stellar (Phillips et al. 2001) plasmas, particularly in the X-ray region (Dere et al. 2001). Additionally, this ion is employed to pump other ions (for example: Li-like iron) in lasing plasmas (Al'Miev et al. 2001). With this in view, we have recently reported (McKeown et al. 2004) energy levels and radiative rates for transitions in Fe XXIV, and here we present our results for all above named parameters for all transitions up to and including the  $n = 5$  levels of Al XIII.

The earlier available atomic data for Al XIII are from our own calculations (Aggarwal et al. 2001), which adopted the  $R$ -matrix program (Berrington et al. 1995) to compute collision strengths ( $\Omega$ ), and also included resonances in threshold region to calculate effective collision strengths ( $\Upsilon$ ). Results were reported for transitions among the  $n \leq 5$  states, but the major deficiency of those results is that the calculations were performed in the  $LS$  coupling scheme. As a result of this, desired atomic data for fine-structure transitions are not available. Therefore, in the present work we are performing a fully relativistic calculation in order to report results for fine-structure transitions. Additionally, we are availing the opportunity to report radiative rates, which are required in any modelling or diagnostic

analysis and are not yet available in the literature. Furthermore, overall improvements are made over the existing (non-relativistic) results by increasing the partial waves range from  $L \leq 45$  to  $J \leq 60$ , energy range for  $\Omega$  from 220 Ryd to 300 Ryd, and the temperature range for  $\Upsilon$  from  $\log T_e \leq 6.4$  K to 6.8 K.

## 2. Atomic structure

The 1s, 2s, 2p, 3s, 3p, 3d, 4s, 4p, 4d, 4f, 5s, 5p, 5d, 5f and 5g configurations of Al XIII give rise to 25 fine-structure levels, listed in Table 1. To calculate energy levels and radiative rates, we have used the GRASP (General purpose Relativistic Atomic Structure Package) code of Dyaal et al. (1989). In Table 1 we list the calculated energies (with and without the inclusion of QED corrections) for these levels. Also included in this table are the experimental energies compiled by NIST (<http://www.physics.nist.gov/PhysRefData>). The net effect of including the QED corrections is to lower the energies by  $\sim 0.027$  Ryd, in general. However, the agreement between the theoretical and experimental level energies is excellent, both in magnitude and orderings.

The absorption oscillator strength ( $f_{ij}$ ) and radiative rate  $A_{ji}$  (in  $s^{-1}$ ) for an allowed transition  $i \rightarrow j$  are related by the following expression:

$$f_{ij} = 1.499 \times 10^{-16} \lambda_{ij}^2 (\omega_j / \omega_i) A_{ji} \quad (1)$$

where  $\lambda_{ij}$  is the transition wavelength in angstroms, and  $\omega_i$  and  $\omega_j$  are the statistical weights of the lower ( $i$ ) and upper ( $j$ ) levels, respectively. In Table 2 we present our calculated values of wavelengths ( $\lambda$  in  $\text{\AA}$ ), oscillator strengths ( $f$ , dimensionless), and radiative rates ( $A$  in  $s^{-1}$ ) for all allowed transitions.

<sup>\*</sup> Tables 2–4 are available only in electronic form at the CDS via anonymous ftp to cdsarc.u-strasbg.fr (130.79.128.5) or via <http://cdsweb.u-strasbg.fr/cgi-bin/qcat?J/A+A/432/1151>

**Table 1.** Comparison between NIST and our present GRASP energy levels (in Ryd) for Al XIII.

Index	Configuration	Level	NIST <sup>a</sup>	GRASP <sup>b</sup>	GRASP <sup>c</sup>
1...	1s	<sup>2</sup> S <sub>1/2</sub>	0.000000	0.000000	0.000000
2...	2s	<sup>2</sup> S <sub>1/2</sub>	126.986288	127.012604	126.988960
3...	2p	<sup>2</sup> P <sup>o</sup> <sub>1/2</sub>	126.982560	127.012604	126.985252
4...	2p	<sup>2</sup> P <sup>o</sup> <sub>3/2</sub>	127.078367	127.108200	127.081062
5...	3p	<sup>2</sup> P <sup>o</sup> <sub>1/2</sub>	150.531340	150.561707	150.534500
6...	3s	<sup>2</sup> S <sub>1/2</sub>	150.532450	150.561707	150.535599
7...	3d	<sup>2</sup> D <sub>3/2</sub>	150.559680	150.590103	150.562851
8...	3p	<sup>2</sup> P <sup>o</sup> <sub>3/2</sub>	150.559700	150.590103	150.562897
9...	3d	<sup>2</sup> D <sub>5/2</sub>	150.569110	150.599503	150.572266
10...	4p	<sup>2</sup> P <sup>o</sup> <sub>1/2</sub>	158.769510	158.800095	158.772842
11...	4s	<sup>2</sup> S <sub>1/2</sub>	158.769980	158.800095	158.773300
12...	4d	<sup>2</sup> D <sub>3/2</sub>	158.781460	158.811996	158.784805
13...	4p	<sup>2</sup> P <sup>o</sup> <sub>3/2</sub>	158.781490	158.811996	158.784821
14...	4d	<sup>2</sup> D <sub>5/2</sub>	158.785450	158.815994	158.788773
15...	4f	<sup>2</sup> F <sup>o</sup> <sub>5/2</sub>	158.785440	158.815994	158.788773
16...	4f	<sup>2</sup> F <sup>o</sup> <sub>7/2</sub>	158.787420	158.817993	158.790756
17...	5s	<sup>2</sup> S <sub>1/2</sub>	162.581180	162.611603	162.584579
18...	5p	<sup>2</sup> P <sup>o</sup> <sub>1/2</sub>	162.580950	162.611603	162.584351
19...	5d	<sup>2</sup> D <sub>3/2</sub>	162.587060	162.617706	162.590469
20...	5p	<sup>2</sup> P <sup>o</sup> <sub>3/2</sub>	162.587070	162.617706	162.590485
21...	5f	<sup>2</sup> F <sup>o</sup> <sub>5/2</sub>	162.589000	162.619705	162.592499
22...	5d	<sup>2</sup> D <sub>5/2</sub>	162.589000	162.619705	162.592499
23...	5g	<sup>2</sup> G <sub>7/2</sub>	162.590100	162.620697	162.593521
24...	5f	<sup>2</sup> F <sup>o</sup> <sub>7/2</sub>	162.590100	162.620697	162.593521
25...	5g	<sup>2</sup> G <sub>9/2</sub>	162.590710	162.621307	162.594131

<sup>a</sup>: NIST (<http://www.physics.nist.gov/PhysRefData>).

<sup>b</sup>: Coulomb energies.

<sup>c</sup>: QED corrected energies.

The indices used to represent a transition have already been given in Table 1. To our knowledge, no other results are available with which to compare. While calculating radiative rates, the QED corrected energies listed in Table 1 have been adopted, and based on the comparison made between the length and velocity forms of the  $f$  (and  $A$ ) values, the accuracy of our results is assessed to be better than 5% for all transitions.

### 3. Collision strengths

For the computations of collision strengths  $\Omega$ , we have adopted the Dirac Atomic  $R$ -matrix Code (DARC) of Norrington & Grant (2005). This program includes relativistic effects in a systematic way, in both the target description and the scattering model. It is based on the  $jj$  coupling scheme, and uses the Dirac-Coulomb Hamiltonian in the  $R$ -matrix approach. In our calculations the  $R$ -matrix radius has been adopted to be 7.36 au, and 55 continuum orbitals have been included for each channel angular momentum for the expansion of the wavefunction. This allows us to compute  $\Omega$  up to an energy of 300 Ryd, which will easily permit us to calculate excitation rate coefficients up to a temperature of  $6.30 \times 10^6$  K, sufficient for applications to a wide variety of plasmas. The maximum number of channels for a partial wave is 110, and the corresponding size of the Hamiltonian matrix is 6088. In order to obtain convergence of  $\Omega$  for all transitions and at all energies, we have included all partial waves with angular momentum  $J \leq 60$ , although a

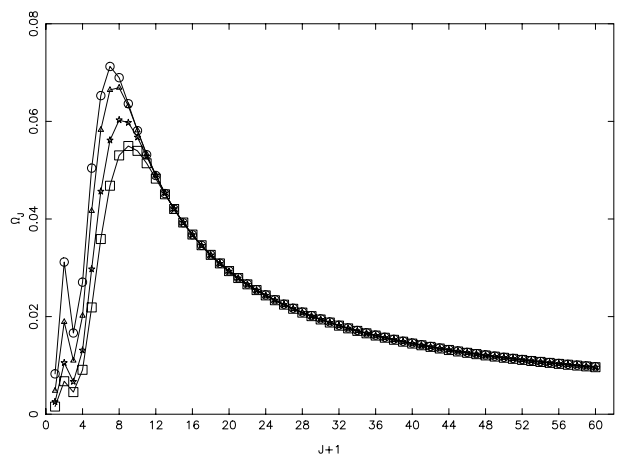


**Fig. 1.** Partial collision strengths for the  $2s^2S_{1/2}-2p^2P^o_{3/2}$  transition (2–4) in Al XIII at 4 electron energies of 170 Ryd (circles), 200 Ryd (triangles), 250 Ryd (stars), and 300 Ryd (squares).

higher range would have been preferable for the convergence of “elastic” transitions (see Fig. 1 above), which are allowed within the degenerate levels of a state.

In Figs. 1–3 we show the variation of  $\Omega$  with angular momentum  $J$  at four energies of 170, 200, 250 and 300 Ryd, and for three transitions, namely 2–4 ( $2s^2S_{1/2}-2p^2P^o_{3/2}$ ), 3–7 ( $2p^2P^o_{1/2}-3d^2D_{3/2}$ ) and 14–22 ( $4d^2D_{5/2}-5d^2D_{5/2}$ ). The 2–4 is an “elastic” transition, which belongs to the degenerate

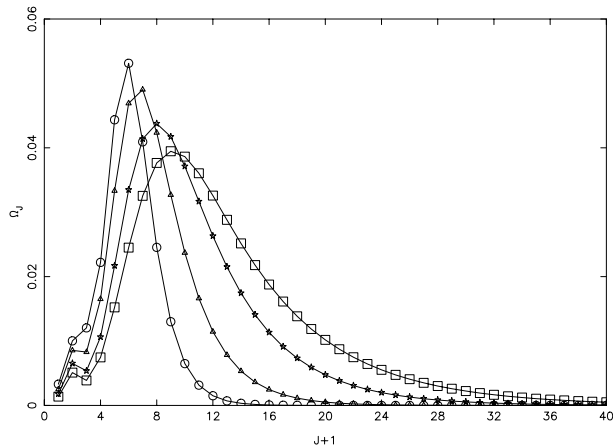


**Fig. 2.** Partial collision strengths for the  $2p^2P^o_{1/2}-3d^2D_{3/2}$  transition (3–7) in Al XIII at 4 electron energies of 170 Ryd (circles), 200 Ryd (triangles), 250 Ryd (stars), and 300 Ryd (squares).

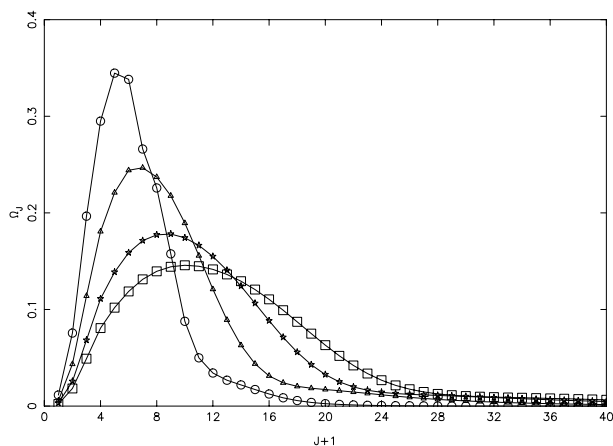


**Fig. 3.** Partial collision strengths for the  $4d^2D_{5/2}-5d^2D_{5/2}$  transition (14–22) in Al XIII at 4 electron energies of 170 Ryd (circles), 200 Ryd (triangles), 250 Ryd (stars), and 300 Ryd (squares).

levels of a state. Such transitions converge very slowly, as seen in Fig. 1, mainly because of their small threshold energies. However, 3–7 is an allowed transition belonging to different  $nl$  levels, but  $\Omega$  for this (and similar other transitions) have fully converged within the partial waves range of our calculations, at all energies. Similarly, the convergence of  $\Omega$  with  $J$  is slow for some forbidden transitions, such as 14–22, as shown in Fig. 3. However, except for the “elastic” transitions discussed above, our values of  $\Omega$  have converged for all other transitions, including the allowed ones, and at all energies.

Our results of  $\Omega$  for “elastic” transitions may be *underestimated* by (over) a factor of two, as can be seen by a comparison with the earlier results of Zygelman & Dalgarno (1987) for the 2–3 and 2–4 transitions. Since the top-up according to the sum rules of Burgess & Tully (1992) results in the overestimation of the contribution of higher neglected partial waves for a majority of allowed (and intercombination) transitions, such as 3–7 transition for which  $\Omega$  has converged within the partial waves range of the calculations as shown in Fig. 2, we have preferred not to apply their sum rule for the elastic transitions. Therefore, our results for  $\Omega$  as well as  $\Upsilon$  (discussed below in

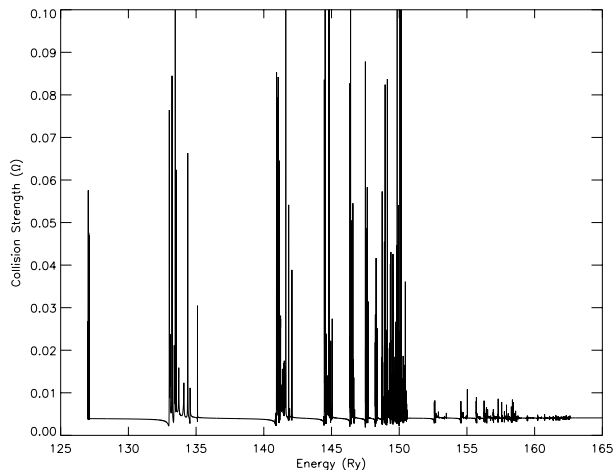


**Fig. 4.** Collision strengths for the  $1s^2S_{1/2}-2s^2S_{1/2}$  transition (1–2) in Al XIII.

Sect. 4) for “elastic” transitions are based on the contribution of partial waves with  $J \leq 60$ , and should be applied with caution.

In Table 3 we list our values of  $\Omega$  for *all* transitions at energies above thresholds. In this energy range the values of  $\Omega$  vary (almost) smoothly, and results at any energy in the  $170.0 \leq E \leq 300.0$  Ryd range can be easily interpolated. The only other results available in the literature with which to compare are our earlier calculations (Aggarwal et al. 2001) performed in the  $LS$  coupling scheme. The present summed-up results for corresponding  $LS$  coupled transitions agree within 10% with our earlier  $\Omega$  values, for all transitions and at all energies. This is highly satisfactory, as expected.

#### 4. Effective collision strengths

Effective collision strengths  $\Upsilon$  are obtained after integrating  $\Omega$  over a Maxwellian distribution of electron velocities, and are very simply related to the excitation  $q(i, j)$  and de-excitation  $q(j, i)$  rate coefficients as shown in Eqs. (1)–(3) of our earlier paper (Aggarwal et al. 2001). In order to account for resonances, we have performed our calculations of  $\Omega$  in a fine energy mesh throughout the thresholds region. Close to thresholds ( $\sim 0.1$  Ryd above each threshold), the energy mesh is 0.001 Ryd, and is 0.002 Ryd in the remaining region. In total, values of  $\Omega$  have been computed at over 18 000 energies in the thresholds region. This fine energy mesh ensures to a large extent that neither a majority of resonances are omitted, nor a few comparatively large resonances have unreasonably large widths. In Figs. 4–6 we demonstrate our results of  $\Omega$  for only three transitions, namely 1–2 ( $1s^2S_{1/2}-2s^2S_{1/2}$ ), 4–6 ( $2p^2P^o_{3/2}-3s^2S_{1/2}$ ), and 9–11 ( $3d^2D_{5/2}-4s^2S_{1/2}$ ). These transitions clearly illustrate the density and importance of resonances. It may also be noted here that although 4–6 is an allowed transition, its resonance structure is quite significant, as seen in Fig. 5.

In Table 4 we list our results of  $\Upsilon$  for all transitions, over a wide temperature range of  $4.4 \leq \log T_e \leq 6.8$  K, which is fully sufficient for applications in laboratory and astrophysical plasmas, but if required, can be extrapolated up to

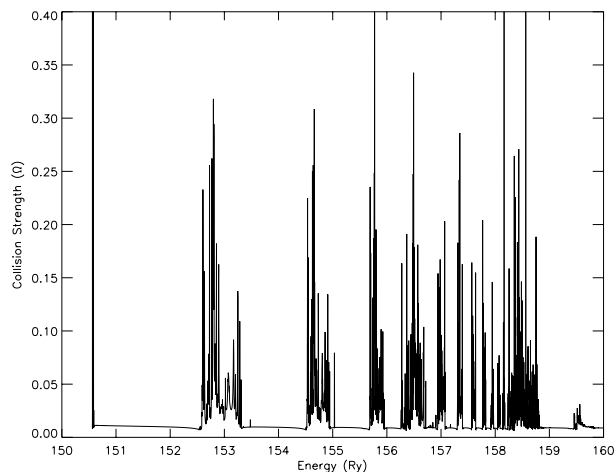


**Fig. 5.** Collision strengths for the  $2p\ 2P_{3/2}^o-3s\ 2S_{1/2}$  transition (4–6) in Al XIII.

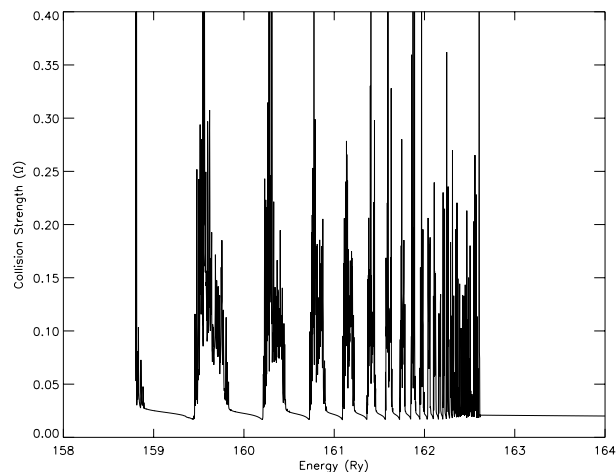


**Fig. 6.** Collision strengths for the  $3d\ 2D_{5/2}-4s\ 2S_{1/2}$  transition (9–11) in Al XIII.

$\log T_e = 7.0$  K without much loss of accuracy. The only other similar results available in the literature are from our earlier non-relativistic calculations (Aggarwal et al. 2001). For a majority of transitions, the agreement between the two sets of calculations is within 10% at all temperatures. However, for four *LS* transitions (with their indices in **bold faces**), namely **1–2** ( $1s\ 2S-2s\ 2S$ ), **2–4** ( $2s\ 2S-3s\ 2S$ ), **2–5** ( $2s\ 2S-3p\ 2P^o$ ), and **6–8** ( $3d\ 2D-4p\ 2P^o$ ), the present results are higher by up to  $\sim 20\%$  towards the lower end of the temperature range, whereas for the **3–7** ( $2p\ 2P^o-4s\ 2S$ ) transition the discrepancy is up to 50%. We show the comparison between the two calculations in Fig. 7 for three transitions, namely **1–2** ( $1s\ 2S-2s\ 2S$ ), **2–4** ( $2s\ 2S-3s\ 2S$ ), and **6–8** ( $3d\ 2D-4p\ 2P^o$ ). As seen in this figure, the differences between the two calculations are only at lower temperatures, and disappear with increasing temperature. The differences at lower temperatures are clearly due to the presence (or absence) of resonances in the thresholds region, as the agreement between the two sets of  $\Omega$  at energies above thresholds is highly satisfactory, as discussed in Sect. 3. Furthermore, a fresh look at Fig. 4 makes these differences clearly understandable. The present Fig. 4 for the **1–2** transition has more (and denser) resonances in comparison to those in Fig. 5 of Aggarwal et al. (2001) for the same transition. The energy mesh in the present work is finer ( $\leq 0.002$  Ryd) in comparison to  $\leq 0.014$  Ryd adopted in our earlier work. In our earlier work, resonances were resolved at  $\sim 3800$  energies in comparison to over 18 000 energies in the present calculations, in the same energy range. However, test calculations with coarser mesh show that it has a negligible effect on the determined values of  $\Upsilon$ , because energy mesh near thresholds is comparable in both calculations, and only differ at energies well above the thresholds. The major differences between the two calculations arise because of the inclusion of fine-structure in the definition of channel coupling, i.e. adoption of the *jj* coupling scheme, which gives rise to additional resonances. The effect of these additional resonances (in the present calculations) is more apparent for three other transitions, which we discuss below.

For three transitions, namely **3–4** ( $2p\ 2P^o-3s\ 2S$ ), **5–7** ( $3p\ 2P^o-4s\ 2S$ ) and **6–7** ( $3d\ 2D-4s\ 2S$ ), differences between our

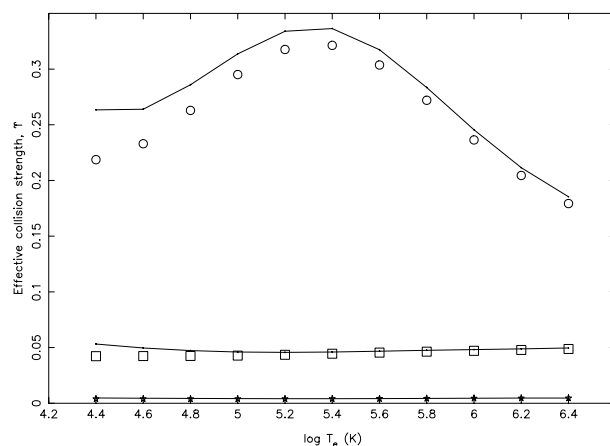


**Fig. 7.** Comparison between present (continuous curve) and earlier (Aggarwal et al. 2001) effective collision strengths for the  $1s\ 2S-2s\ 2S$  (**1–2**: stars and the lowest curve),  $2s\ 2S-3s\ 2S$  (**2–4**: squares and the middle curve), and  $3d\ 2D-4p\ 2P^o$  (**6–8**: circles and the upper curve) transitions in Al XIII.

present and earlier (Aggarwal et al. 2001) results of  $\Upsilon$  are up to a factor of three as shown in Fig. 8. At lower temperatures the present results are invariably higher, and merge with the earlier results with increasing temperature. Since the discrepancy is highest for the **3–4** transition, we discuss this transition in further detail to understand the differences. A closer look at Fig. 5 for the **4–6** ( $2p\ 2P_{3/2}^o-3s\ 2S_{1/2}$ ) transition clearly shows that resonances are denser (and some of them are higher in magnitude as well), in comparison to those shown in Fig. 9a of Aggarwal et al. (2001) for the corresponding *LS* transition. Additionally, very close to the threshold there are a few narrow resonances, which were not there in the earlier work. As a result of these, the present results of  $\Upsilon$  are considerably higher towards the lower end of the temperature range. In fact the same conclusion applies to the **5–7** and **6–7** transitions, as can be seen in Fig. 6 for the **9–11** ( $3d\ 2D_{5/2}-4s\ 2S_{1/2}$ ) transition, which is a part of the **6–7** transition in *LS* coupling. However, to confirm the effect of these (few) near threshold resonances, we have performed an exercise by re-calculating

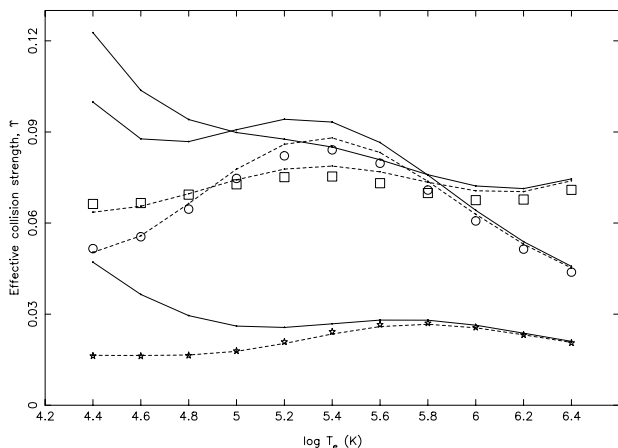


**Fig. 8.** Comparison between present (continuous curve) and earlier (Aggarwal et al. 2001) effective collision strengths for the  $2p^2P^o-3s^2S$  (3–4: stars and the lowest curve),  $3p^2P^o-4s^2S$  (5–7: squares and the upper curve), and  $3d^2D-4s^2S$  (6–7: circles and the middle curve) transitions in Al XIII. The results obtained *without* near threshold resonances (see Sect. 4) are shown as broken curves.

values of  $\Upsilon$  *without* them. The results so obtained are also shown in Fig. 8 as broken lines. As expected, the agreement between the two calculations is excellent (within 5%) at all temperatures. Therefore, inclusion of additional resonances (arising from the redistribution of levels ordering as shown in Table 1) has affected the values of  $\Upsilon$  for a few transitions, particularly at lower temperatures. This is a very interesting conclusion, as it emphasizes the importance of relativistic effects in a calculation for a comparatively light ion, such as Al XIII.

## 5. Discussion and conclusions

In this paper we have reported results for energy levels, radiative rates, collision strengths and effective collision strengths for transitions in Al XIII. Apart from the inclusion of relativistic effects to calculate our results for fine-structure transitions, a few other improvements have been made over our earlier (non-relativistic) results (Aggarwal et al. 2001), which are: (i) the partial waves range has been increased from 45 to 60, which improves the convergence of  $\Omega$  for allowed transitions, particularly at higher energies; (ii) the energy range has been increased from 220 to 300 Ryd, which enabled us to increase the temperature range of  $\Upsilon$  from  $2.5 \times 10^6$  K to  $6.3 \times 10^6$  K; and (iii) the energy mesh is finer in the thresholds region from  $\leq 0.014$  Ryd to  $\leq 0.002$  Ryd, which has improved the accuracy of  $\Upsilon$  results, particularly at lower temperatures. Additionally, radiative rates have been reported for transitions among the  $n \leq 5$  levels of Al XIII, which were not available earlier.

Since our earlier non-relativistic calculations for Al XIII are already available in the literature (Aggarwal et al. 2001), two definite conclusions can be drawn from the comparison with present relativistic results. Firstly, relativistic effects are very important, because inclusion of fine-structure in the definition of channel coupling gives rise to additional resonances, and hence increases the value of  $\Upsilon$  by up to a factor of three, for some of the transitions, particularly at lower

temperatures. Secondly, in a non-relativistic calculation, results for  $\Omega$  and  $\Upsilon$  for fine-structure transitions can be derived from the corresponding  $LS$  transition, if one of the levels is non-degenerate, such as  $^2S$  and  $^1D$ , because of the following statistical relationship:

$$\Upsilon \left( {}^{2S+1}L_J - {}^{2S'+1}L'_{J'} \right) = \frac{(2J+1)}{(2S+1)(2L+1)} \Upsilon \left( {}^{2S+1}L - {}^{2S'+1}L' \right). \quad (2)$$

In the present calculations, the above relationship is (generally) true for values of  $\Omega$  – see, for example, 1–3,4; 2–3,4; and 6–7, 9 transitions in Table 3. For a majority of such transitions, the above relationship is also true for the  $\Upsilon$  values, but it is not true for a few transitions, such as: 2–3 and 2–4, particularly at lower temperatures. This is because of the (non-proportionate) contribution of resonances, which affects the  $\Upsilon$  values more at lower temperatures than the higher ones, as can also be seen in Table 4. This anomaly could have important implication if such transitions are of particular interest.

Finally, the atomic data reported in this paper are probably the best available to date, and we hope the present set of results will be highly useful for diagnostic and modelling applications. The accuracy of our energy levels and radiative rates are assessed to be better than 1% and 5%, respectively, whereas the corresponding results for  $\Omega$  and  $\Upsilon$  could easily vary by up to 20% at higher energies and lower temperatures, respectively. Furthermore, our  $\Upsilon$  results for transitions involving the  $n = 5$  levels may be comparatively less accurate, particularly at lower temperatures, because resonances arising from the  $n \geq 6$  levels have not been included in the present work.

*Acknowledgements.* The work reported in this paper has been financed by the EPSRC and PPARC of the United Kingdom. We wish to thank Dr. Patrick Norrington for providing his code prior to publication. FPK and SJR (©British Crown Copyright 2004/Mod) are grateful to AWE Aldermaston for the award of William Penney Fellowships. Finally, we thank an anonymous Referee for his useful comments and suggestions.

## References

- Aggarwal, K. M., Keenan, F. P., & Rose, S. J. 2001, *Phys. Scr.*, 63, 95
- Al'Miev, I. R., Rose, S. J., & Wark, J. S. 2001, *J. Quant. Spectros. Radiat. Transfer*, 71, 129
- Berrington, K. A., Eissner, W. B., & Norrington, P. H. 1995, *Comput. Phys. Commun.*, 92, 290
- Burgess, A., & Tully, J. A. 1992, *A&A*, 254, 436
- Dere, K. P., Landi, E., Young, P. R., & Del Zanna, G. 2001, *ApJS*, 134, 331
- Dyall, K. G., Grant, I. P., Johnson, C. T., Parpia, F. A., & Plummer, E. P. 1989, *Comput. Phys. Commun.*, 55, 424
- McKeown, K., Aggarwal, K. M., Keenan, F. P., & Rose, S. J. 2004, *Phys. Scr.*, 70, 295
- Norrington, P. H., & Grant, I. P. 2005, *Comput. Phys. Commun.*, in preparation
- Phillips, K. J. H., Fawcett, B. C., Kent, B. J., et al. 1982, *ApJ*, 256, 774
- Phillips, K. J. H., Mathioudakis, M., Huenemörder, M., et al. 2001, *MNRAS*, 325, 1500
- Zygelman, B., & Dalgarno, A. 1987, *Phys. Rev. A* 35, 4085